Journal of Sound and Vibration (1997) **207**(3), 301–317

THE RESPONSE OF AND SOUND POWER RADIATED BY A CLAMPED RECTANGULAR PLATE

C.-C. Sung and J. T. Jan

Department of Naval Architecture and Ocean Engineering, National Taiwan University, Taiwan, Republic of China

(*Received* 3 *October* 1995, *and in final form* 29 *April* 1997)

The dynamic response of a clamped vibrating rectangular plate excited by steady-state harmonic point forces, couples and piezomoments are derived, based on a new method. This method eliminates the difficulties involved in solving high order simultaneous equations/matrices and provides an easier approach to calculating the structurally radiated sound. Point force and piezomoment inputs are experimentally applied by using electromagnetic shaker and piezoceramic excitors attached to the surface of the plate. The coupling effect due to the bounding layer between the plate and the piezoceramic actuators is also determined. The sound radiation measurement is conducted in a reverberant room equipped with an anechoic chamber. Results from these experiments indicate that the proposed method provides an accurate and efficient approach for theoretical estimation of the response of clamped rectangular plates and the structurally radiated sound power.

1. INTRODUCTION

Sound radiation emitted by a vibrating plate is encountered very often. The sound power radiated by such a plate can be calculated if its surface response is known. A number of studies have been devoted to the derivation of plate response with various boundary conditions. For simply supported plates the solution is easier to obtain [1]. However, for a plate which is not simply supported, e.g., clamped–clamped, clamped–elastically supported and clamped–simply supported etc., the solution becomes much more complex. Both the methods, viz., Ritz [2] and superposition [3], which are widely used, have to solve high order simultaneous equations or high order matrices, making the calculations of structurally radiated sound power even more difficult. Based on Galerkin's method, Vlasov proposed a solution [4] in 1949 for clamped or simply supported rectangular plates under static load. In the present work, the dynamic response of a clamped or elastically supported plate subjected to various excitations, e.g., piezoactuators, is calculated. The Rayleigh integral expression [5] has been employed to obtain the sound pressure distribution and radiated sound power. Optimized control forces for minimization or radiated sound are easier to achieve by the present approach.

A 40 cm × 40 cm clamped steel plate with a 2 mm thickness was used for the experiment. The response of the plate was measured by using an electromagnatic shaker and piezoceramic excitors. The weight of the piezoceramic actuators which were bonded directly to the plate surface, can be neglected compared to the weight of the steel plate [6–8]. The linearity of the piezoceramic excitors and the bonding layer was experimentally verified for the range of testing frequencies. The radiated sound power measurement was conducted in the reverberant room equipped with an anechoic chamber to simulate the

0022–460X/97/430301 + 17 $25.00/0/sv971125

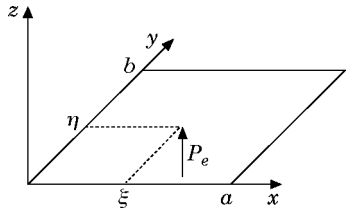

Figure 1. Co-ordinate system of the plate.

TABLE 1

Comparisons between the natural frequencies of the clamped plate bonded by four piezoceramic patches

	Natural frequencies (Hz)			
Mode	Rayleigh-Ritz	present	experimental measurements for plate bonded by four PZT patches	error between column (2) and (3) (%)
1	106·88	107·24	106	1·2
2	217·98	219·20	214·45	2·2
3	321·42	324·29	319	1·7
4	390·81	396·37	389	1·9
5	392·66	396·37	390·8	1·4
6	490·07	502·13	489	2·7

semi-infinite free space. The results for the calculated and measured sound power was observed to match perfectly after the acoustic absorbing condition for the opening of the anechoic chamber was improved. This indicates that the present method can be successfully used to predict the plate response and radiated sound power.

2. SOLUTION FOR FORCED VIBRATIONS OF A CLAMPED PLATE

For an undamped thin plate under the external excitation force $P_e(x, y, t)$, shown in Figure 1, the governing equation of bending vibrations is

$$D\left(\frac{\partial^4}{\partial x^4} + 2\frac{\partial^4}{\partial x^2\,\partial y^2} + \frac{\partial^4}{\partial y^4}\right)w(x, y, t) + \rho_s h\frac{\partial^2 w(x, y, t)}{\partial t^2} = p_e(x, y, t), \tag{1}$$

where $w(x, y, t)$ is the displacement along z direction at the point (x, y),

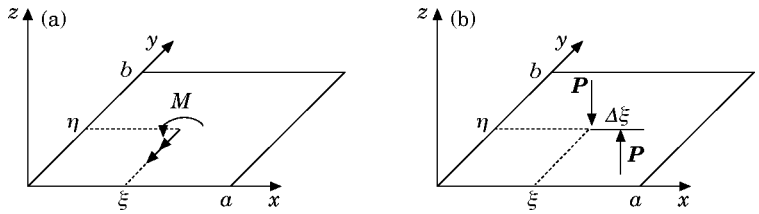

Figure 2. Plate under the excitation by (a) single concentrated moment (b) two concentrated forces to simulate single concentrated moment.

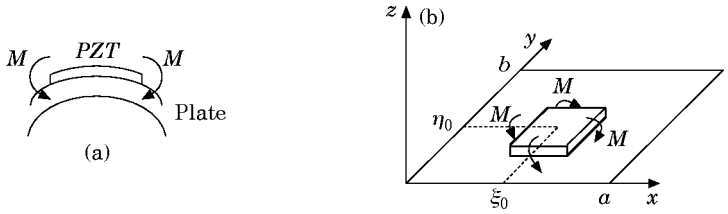

Figure 3. Plate under the excitation by four concentrated moments simulating a piezo actuator.

$D = Eh^3/12(1 - v^2)$, E is Young's modulus, h is the plate thickness, v is Poisson's ratio and ρ is the density of the plate.

Consider the external force P_e to be a harmonic point force with frequency ω acting on the point (ξ, η), along the positive z-axis and let

$$w(x, y, t) = W(x, y)\, e^{i\omega t}, \qquad p_e(x, y, t) = P(x, y)\, e^{i\omega t}. \tag{2}$$

Substituting equation (2) into equation (1), the governing equation can be simplified as

$$D\left(\frac{\partial^4}{\partial x^4} + 2\frac{\partial^4}{\partial x^2\,\partial y^2} + \frac{\partial^4}{\partial y^4}\right)W(x, y) - \bar{m}\omega^2 W(x, y) - P(x, y) = 0, \tag{3}$$

where $\bar{m} = \rho_s h$ is the area density of the plate.

Expanding $W(x, y)$ and $P(x, y)$ as the superposition of adequate shape functions, one obtains

$$W(x, y) = \sum_{m=1}^{\infty}\sum_{n=1}^{\infty} W_{mn}\phi_{mn}(x, y), \qquad P(x, y) = \sum_{m=1}^{\infty}\sum_{n=1}^{\infty} P_{mn}\psi_{mn}(x, y). \tag{4a, b}$$

The Virtual Work Principle is given as

$$\int_0^b \int_0^a [D\nabla^2\nabla^2 W(x, y) - \bar{m}\omega^2 W(x, y) - P(x, y)](\delta W)\, dx\, dy = 0, \tag{5}$$

where the virtual displacement δW is written as

$$\delta W = \sum_{i=1}^{\infty}\sum_{k=1}^{\infty} \delta W_{ik}\phi_{ik}(x, y), \qquad \text{and} \qquad \nabla^2\nabla^2 = \frac{\partial^4}{\partial x^4} + 2\frac{\partial^4}{\partial x^2\,\partial y^2} + \frac{\partial^4}{\partial y^4}.$$

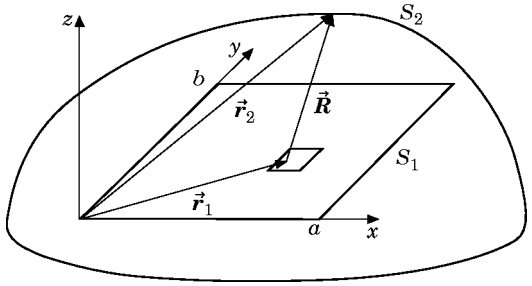

Figure 4. Integration areas S_1 and S_2 for the calculation of sound power radiated by plate.

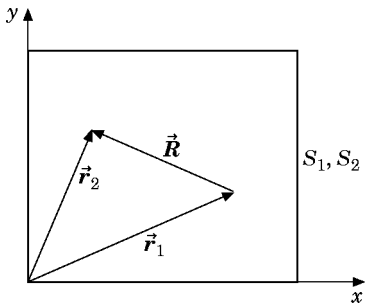

Figure 5. Integration areas for sound power for $S_1 = S_2$.

The shape functions in equation (4) can be further decomposed as

$$\phi_{mn}(x, y) = \psi_{mn}(x, y) = X_m(x)Y_n(y) \tag{6}$$

Eigenfunctions $X_m(x)$ and $Y_n(y)$ have been chosen such that both of them satisfy the boundary conditions for the plate. Equation (4b) then becomes the Fourier series expansion of $P(x, y)$ and P_{mn} can be expressed as

$$P_{mn} = \int_0^b \int_0^a P(x, y)X_m(x)Y_n(y)\,\mathrm{d}x\,\mathrm{d}y \Big/ \int_0^b \int_0^a X_m^2(x)Y_n^2(y)\,\mathrm{d}x\,\mathrm{d}y. \tag{7}$$

Substituting equation (4a) and (4b) into equation (5), one obtains

$$D\sum_{\substack{m\\i}}^{\infty}\sum_{\substack{n\\k}}^{\infty} W_{mn}\int_0^b\int_0^a \phi_{ik}\nabla^2\nabla^2\phi_{mn}\,\mathrm{d}x\,\mathrm{d}y - \bar{m}\omega^2\sum_{\substack{m\\i}}^{\infty}\sum_{\substack{n\\k}}^{\infty} W_{mn}\int_0^b\int_0^a \phi_{ik}\phi_{mn}\,\mathrm{d}x\,\mathrm{d}y$$

$$-\sum_{\substack{m\\i}}^{\infty}\sum_{\substack{n\\k}}^{\infty} P_{mn}\int_0^b\int_0^a \phi_{ik}\psi_{mn}\,\mathrm{d}x\,\mathrm{d}y = 0. \tag{8}$$

Using equation (6), equation (8) can be converted into

$$D\sum_{\substack{m\\i}}\sum_{\substack{n\\k}} W_{mn}\int_0^b\int_0^a [X_m^{(4)}Y_nX_iY_k + 2X_m''Y_n''X_iY_k + Y_n^{(4)}X_mX_iY_k]\,\mathrm{d}x\,\mathrm{d}y$$

$$-\bar{m}\omega^2\sum_{\substack{m\\i}}\sum_{\substack{n\\k}} W_{mn}\int_0^b\int_0^a X_mY_nX_iY_k\,\mathrm{d}x\,\mathrm{d}y$$

$$=\sum_{\substack{m\\i}}^{\infty}\sum_{\substack{n\\k}}^{\infty}\frac{\displaystyle\int_0^b\int_0^a P(x, y)X_m(x)Y_n(y)\,\mathrm{d}x\,\mathrm{d}y}{\displaystyle\int_0^b\int_0^a X_m^2(x)Y_n^2(y)\,\mathrm{d}x\,\mathrm{d}y}\int_0^b\int_0^a X_mY_nX_iY_k\,\mathrm{d}x\,\mathrm{d}y. \tag{9}$$

The eigenfunctions $X_m(x)$, $Y_n(y)$ and $X_i(x)$, $Y_k(y)$ are, respectively, orthogonal to each other such that

$$\left.\begin{aligned}\int_0^a X_p(x)X_q(x)\,\mathrm{d}x = \int_0^a X_p''(x)X_q''(x)\,\mathrm{d}x = 0\\ \int_0^b Y_p(y)Y_q(y)\,\mathrm{d}y = \int_0^b Y_p''(y)Y_q''(y)\,\mathrm{d}y = 0\end{aligned}\right\}, \qquad \text{if } p \neq q.$$

Equation (9) can now be simplified as

$$D\sum_m\sum_n W_{mn}(I_1I_2 + 2I_3I_4 + I_5I_6) - \bar{m}\bar{\omega}^2\sum_m\sum_n W_{mn}I_2I_6 = \sum_m\sum_n\int_0^b\int_0^a P(x,y)X_mY_n\,\mathrm{d}x\,\mathrm{d}y, \tag{10}$$

where,

$$I_1 = \int_0^a X_m^{(4)}X_m\,\mathrm{d}x, \qquad I_4 = \int_0^b Y_n''Y_n\,\mathrm{d}y, \qquad I_2 = \int_0^b Y_n^2\,\mathrm{d}y,$$

$$I_5 = \int_0^b Y_n^{(4)}Y_n\,\mathrm{d}y, \qquad I_3 = \int_0^a X_m''X_m\,\mathrm{d}x, \qquad I_6 = \int_0^a X_m^2\,\mathrm{d}x.$$

Therefore,

$$W_{mn} = \int_0^b\int_0^a P(x,y)X_mY_n\,\mathrm{d}x\,\mathrm{d}y \Big/ (D(I_1I_2 + 2I_3I_4 + I_5I_6) - \bar{m}\omega^2I_2I_6). \tag{11}$$

For a concentrated load, $P(x, y) = P\,\delta(x-\xi)\,\delta(y-\eta)$, then

$$W_{mn} = PX_m(\xi)Y_n(\eta)/D(I_1I_2 + 2I_3I_4 + I_5I_6) - \bar{m}\omega^2I_2I_6). \tag{11a}$$

The dynamic response $W(x, y)$ of the plate subjected to a harmonic point force can thus be expressed as

$$W(x,y) = \sum_m^\infty\sum_n^\infty \frac{PX_m(\xi)Y_n(\eta)}{D(I_1I_2 + 2I_3I_4 + I_5I_6) - \bar{m}\omega^2I_2I_6)}X_m(x)Y_n(y). \tag{12}$$

The shape functions $X_m(x)$ and $Y_n(y)$ can be arbitrarily chosen as long as they are quasi-orthogonal and satisfy the boundary conditions. Consider a beam of length l, the equation of motion can be written as

$$EI\,\partial^4w(x,y)/\partial x^4 + m\,\partial^2w(x,t)/\partial t^2 = 0, \tag{13}$$

where EI and m are the flexural rigidity and mass per unit length respectively. Let $w(x, t) = X(x)\sin(\omega t)$, and substituting this into equation (13) one obtains

$$X_m(x) = C_1\sin\frac{\lambda_m x}{1} + C_2\cos\frac{\lambda_m x}{1} + C_3\sinh\frac{\lambda_m x}{1} + C_4\cosh\frac{\lambda_m x}{1}, \tag{14}$$

where C_1, C_2, C_3 and C_4 are determined by the boundary conditions and λ_m is the eigenvalue of the mth mode. The selection of $Y_n(y)$ is the same as that for $X_m(x)$.

The normal velocity at the surface point (x, y) is obtained as

$$v(x, y, t) = \partial w(x, y, t)/\partial t = \mathrm{i}\omega W(x, y)\, \mathrm{e}^{\mathrm{i}\omega t} = \omega W(x, y)\, \mathrm{e}^{\mathrm{i}(\omega t + \pi/2)},$$

which can be rewritten as

$$v(x, y, t) = V(x, y)\, \mathrm{e}^{\mathrm{i}(\omega t + \pi/2)}, \tag{15}$$

where $V(x, y)$ is the magnitude of $v(x, y, t)$.

Using equation (11), the natural frequencies ω_{mn} can be found by allowing the denominator of

$$W_{mn} = \int_0^b \int_0^a P(x, y) X_m Y_n \, \mathrm{d}x \, \mathrm{d}y \Big/ (D(I_1 I_2 + 2I_3 I_4 + I_5 I_6) - \bar{m}\omega^2 I_2 I_6)$$

to be zero. Thus,

$$\omega_{mn} = \sqrt{D(I_1 I_2 + 2I_3 I_4 + I_5 I_6)/\bar{m} I_2 I_6} \tag{16}$$

In order to verify equation (16), two cases are evaluated and compared:

1. Choosing eigenfunctions for simply supported boundaries [9]

   $$X_m(x) = \sin(m\pi x/a), \qquad Y_n(y) = \sin(n\pi y/b)$$

   and substituting into equation (16), the natural frequencies are obtained as

   $$\omega_{mn} = \pi^2(m^2/a^2 + n^2/b^2)\sqrt{D/\bar{m}}. \tag{17}$$

   These results are identical to those shown in [2].
2. Choosing eigenfunctions for a beam clamped on both ends [9] and calculating the natural frequencies for clamped plates.

   $$X_m(x) = J(\lambda_m x/a) - [J(\lambda_m)/H(\lambda_m)]H(\lambda_m x/a)$$

   and

   $$Y_n(y) = J(\lambda_n y/b) - [J(\lambda_n)/H(\lambda_n)]H(\lambda_n y/b)$$

where

$$J(u) = \cosh(u) - \cos(u)$$
$$H(u) = \sinh(u) - \sin(u)$$

and λ_m and λ_n satisfy $\cosh(\lambda)\cos(\lambda) = 1$. The results obtained by substituting $X_m(x)$ and $Y_n(y)$ into equation (16) are compared with the results reported in reference 13 in Table 1.

A point moment can be treated as two point forces with the same magnitude but separated by a distance $\Delta\xi$ and oriented along opposite direction with respect to each other [2]. Consider a point moment M acting on the plate at point (ξ, η), as shown in Figure 2(a), then M can be represented as

$$M = \mathbf{M}\, \delta(x - \xi)\delta(y - \eta)\, \mathrm{e}^{\mathrm{i}\omega t}, \tag{19}$$

where $\mathbf{M}$ is the magnitude of M and delta function δ is defined as

$$\delta(x - \xi) = \begin{cases} 1, & x = \xi, \\ 0, & x \neq \xi. \end{cases}$$

When a point moment $\mathbf{M}$ is substituted by a couple and letting $\mathbf{M} = \mathbf{P}(\Delta\xi)$, the total response of the plate will be the superposition of the responses induced by the two point forces;

$$W(x, y) = \mathbf{P}\left[\lim_{\Delta\xi\to 0} f(\xi + \Delta\xi, \eta, x, y) - f(\xi, \eta, x, y)\right], \tag{20}$$

where $f(\xi, \eta)$ and $f(\xi + \Delta\xi, \eta)$ represent the responses induced by the two unit point forces located at (ξ, η) and $(\xi + \Delta\xi, \eta)$ respectively.

Let $\Delta\xi$ approach zero and keep $\mathbf{M} = \mathbf{P}(\Delta\xi)$ constant, then $\mathbf{P}$ approaches infinity. Then equation (20) becomes

$$W(x, y) = \mathbf{M}\left[\lim_{\Delta\xi\to 0} [f(\xi + \Delta\xi, \eta, x, y) - f(\xi, \eta, x, y)]/\Delta\xi\right]. \tag{21}$$

Using equation (21), equation (12) can be written as

$$W(x, y) = \sum_m \sum_n \left[\frac{\mathbf{M}X_m(x)Y_n(y)Y_n(\eta)}{D(I_1I_2 + 2I_3I_4 + I_5I_6) - \bar{m}\omega^2 I_2 I_6}\frac{\partial X_m(\xi)}{\partial\xi}\right]. \tag{22}$$

Equation (22) represents the response of the plate to excitation by the point moment acting along the negative y direction. Similarly, when the moment is applied along the x direction, the plate response is obtained as

$$W(x, y) = \sum_m \sum_n \left[\frac{\mathbf{M}X_m(x)Y_n(y)X_m(\xi)}{D(I_1I_2 + 2I_3I_4 + I_5I_6) - \bar{m}\omega^2 I_2 I_6}\frac{\partial Y_n(\eta)}{\partial\eta}\right]. \tag{23}$$

Consider a piezoceramic actuator perfectly bonded on the plate. When an alternating electric field is applied on the piezoceramic actuator along the z direction, the induced strain along the x and y directions will cause the plate to vibrate. This excitation can be treated as four point moments concentrated on the midpoint of four edges of the piezoceramic actuator (Figure 3(a)). The piezoceramic actuator is a square patch with each side of length l.

From equation (22) and equation (23), and by considering the plate response induced by the piezoceramic actuator to be the superposition of the responses induced by four point moments, one gets

$$W(x, y) = \sum_m \sum_n \frac{\mathbf{M}X_m(x)Y_n(y)}{D(I_1I_2 + 2I_3I_4 + I_5I_6) - \bar{m}\omega^2 I_2 I_6}\left[Y_n(\eta)\frac{\partial X_m(\xi)}{\partial\xi}\bigg|_{\substack{\xi=\xi_0-\frac{1}{2}\\ \eta=\eta_0}}\right.$$

$$\left. - Y_n(\eta)\frac{\partial X_m(\xi)}{\partial\xi}\bigg|_{\substack{\xi=\xi_0+\frac{1}{2}\\ \eta=\eta_0}} + X_m(\xi)\frac{\partial Y_n(\eta)}{\partial\eta}\bigg|_{\substack{\xi=\xi_0\\ \eta=\eta_0-\frac{1}{2}}} - X_m(\xi)\frac{\partial Y_n(\eta)}{\partial\eta}\bigg|_{\substack{\xi=\xi_0\\ \eta=\eta_0+\frac{1}{2}}}\right]. \tag{24}$$

The bonding layer between the piezoceramic patch and the plate is ass*umed to be linear*. *The relation between the piezomoment M and the applied voltage* ε_{PZT}, according to equations (19) and (24), is then assumed to be

$$M = k_0\varepsilon_{PZT}. \tag{25}$$

3. CALCULATION OF THE SOUND POWER RADIATED BY THE PLATE

During the vibration of the plate, the normal velocity of the acoustic medium on the surface of the plate loaded at $\vec{\mathbf{r}}_1$ has to be equal to the normal velocity of the plate $v(\vec{\mathbf{r}}_1)$ in order to satisfy the requirement of continuity as shown in Figure 4. Due to the acoustic perturbation on the surface of the plate, the acoustic pressure $P(\vec{\mathbf{r}}_2)$ at $\vec{\mathbf{r}}_2$ is created and can be obtained by Rayleigh's integral [5]

$$P(\vec{\mathbf{r}}_2) = \frac{\omega\rho_f}{2\pi}\int_{S_1} v(\vec{\mathbf{r}}_1)\frac{\mathrm{e}^{-\mathrm{i}kR}}{R}\,\mathrm{d}S_1, \tag{26}$$

where ω is the angular frequency of the plate, k is the wave number, ρ_f is the density of air, R is the distance between points $\vec{\mathbf{r}}_1$ and $\vec{\mathbf{r}}_2$, i.e., $R = |\vec{\mathbf{r}}_1 - \vec{\mathbf{r}}_2|$, and S_1 is the area of the plate.

The acoustic intensity $I(\vec{\mathbf{r}}_2)$ at $\vec{\mathbf{r}}_2$ can be expressed as,

$$I(\vec{\mathbf{r}}_2) = \tfrac{1}{2}\mathrm{Re}\,\{P(\vec{\mathbf{r}}_2)v^*(\vec{\mathbf{r}}_2)\}, \tag{27}$$

where $v(\vec{\mathbf{r}}_2)$ is the normal velocity of the acoustic medium at $\vec{\mathbf{r}}_2$ and * denotes its complex conjugate.

The sound power W_P radiated into the semi-infinite space above the plate is

$$W_p = \int_{S_2} I(\vec{\mathbf{r}}_2)\,\mathrm{d}S_2, \tag{28}$$

when S_2 is an arbitrary surface which covers area S_1 and $\vec{\mathbf{r}}_2$ is the position vector of S_2 (see Figure 4).

Substituting equations (26) and (27) into equation (28) and allowing $S_2 = S_1$, then $\vec{\mathbf{r}}_1$ and $\vec{\mathbf{r}}_2$ would represent any two arbitrary position vectors on the surface of the plate (see Figure 5). The power radiated by the plate can then be expressed as

$$W_P = \frac{\omega\rho_f}{4\pi}\int_{S_2}\int_{S_1}\mathrm{Re}\left\{v(\vec{\mathbf{r}}_1)\cdot\left(\frac{\mathrm{i}\,\mathrm{e}^{-\mathrm{i}kR}}{R}\right)\cdot v^*(\vec{\mathbf{r}}_2)\right\}\mathrm{d}S_1\,\mathrm{d}S_2, \tag{29}$$

where S_1 and S_2 are areas on the x-y plane with $0 < x < a$ and $0 < y < b$.

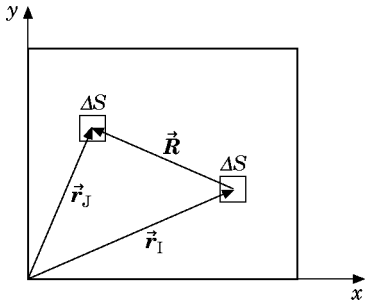

Figure 6. Discretization of plate area.

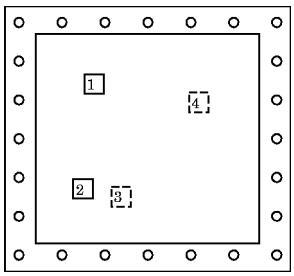

Figure 7. Setup of clamped square plate and the positions of four bonded piezoceramics (piezoceramics on the back of the plate have been shown by dotted lines).

For an arbitrary complex function $\mathbf{C}$, the relation $\mathrm{Re}\{\mathbf{C}\} = \mathbf{C} + \mathbf{C}^*/2$ is always valid. Therefore equation (29) can be expanded as,

$$\mathrm{Re}\left\{\mathrm{v}(\check{\mathbf{r}}_1)\cdot\left(\frac{\mathrm{i}\,\mathrm{e}^{-\mathrm{i}kR}}{R}\right)\cdot v^*(\check{\mathbf{r}}_2)\right\} = \frac{1}{2}\left\{\left[v(\check{\mathbf{r}}_1)\cdot\left(\frac{\mathrm{i}\,\mathrm{e}^{-\mathrm{i}kR}}{R}\right)\cdot v^*(\check{\mathbf{r}}_2)\right]\right.$$

$$\left.+\left[v^*(\check{\mathbf{r}}_1)\cdot\left(\frac{-\mathrm{i}\,\mathrm{e}^{-\mathrm{i}kR}}{R}\right)\cdot v(\check{\mathbf{r}}_2)\right]\right\}$$

$$= \frac{1}{2}\left\{\left[v(\check{\mathbf{r}}_1)\cdot\left(\frac{\sin\theta + \mathrm{i}\cos\theta}{R}\right)\cdot v^*(\check{\mathbf{r}}_2)\right]\right.$$

$$\left.+\left[v^*(\check{\mathbf{r}}_1)\cdot\left(\frac{\sin\theta - \mathrm{i}\cos\theta}{R}\right)\cdot v(\check{\mathbf{r}}_2)\right]\right\}. \tag{30}$$

Due to the reciprocity relation between source at $\check{\mathbf{r}}_1$ and receiver at $\check{\mathbf{r}}_2$, equation (30) can be simplified as

$$\mathrm{Re}\left\{v(\check{\mathbf{r}}_1)\cdot\left(\frac{\mathrm{i}\,\mathrm{e}^{-\mathrm{i}kR}}{R}\right)\cdot v^*(\check{\mathbf{r}}_2)\right\} = v(\check{\mathbf{r}}_1)\cdot\left(\frac{\sin(kR)}{R}\right)\cdot v^*(\check{\mathbf{r}}_2) \tag{31}$$

and thus equation (29) becomes

$$W_P = \frac{\omega\rho_f}{4\pi}\int_0^b\int_0^a\left[\int_0^b\int_0^a v(\check{\mathbf{r}}_1)\cdot\left(\frac{\sin(kR)}{R}\right)\cdot v^*(\check{\mathbf{r}}_2)\,\mathrm{d}x_1\,\mathrm{d}y_1\right]\mathrm{d}x_2\,\mathrm{d}y_2. \tag{32}$$

Consider the rectangular plate to be divided into N elements and the area of each element to be ΔS (See Figure 6), equation (32) can then be approximated as a finite series

$$W_P \cong \frac{\omega\rho_f}{4\pi}\sum_J\sum_I\frac{\sin(kR)}{R}\,v(\check{\mathbf{r}}_1)\cdot v^*(\check{\mathbf{r}}_J)(\Delta S)\cdot(\Delta S), \tag{33}$$

where $\check{\mathbf{r}}_I$ and $\check{\mathbf{r}}_J$ are the position vectors of the center point of two arbitrary elements, and $R = |\check{\mathbf{r}}_I - \check{\mathbf{r}}_J|$.

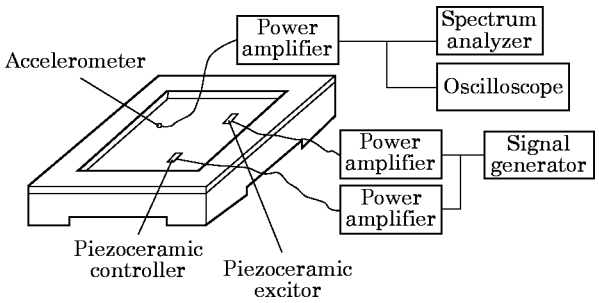

Figure 8. The experimental setup for the measurement of plate response.

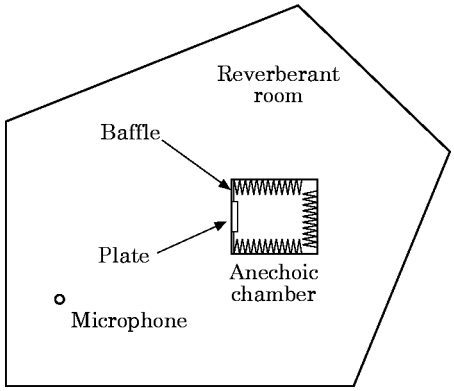

Figure 9. The experimental setup for the measurement of plate radiation power in a reverberant room with an anechoic chamber.

4. MEASUREMENTS OF SOUND POWER RADIATED BY A PLATE IN A REVERBERANT ROOM

The measurements were performed on a 40 cm × 40 cm × 2 mm thick rectangular steel plate. The boundary was a rectangular steel frame. The plate was clamped onto the frame by four 2 cm thick steel bars with screws every 5 cm apart (Figure 7). The total weight of the frame along with 4 bars was 40 kg.

Piezoceramic patches 1 and 2 were bonded on the upper surface at locations (8·7, 11·5) cm, (11·3, 31) cm, respectively, whereas piezoceramic patches 3 and 4 are bonded on the lower surface at locations (13·8, 11) cm, (26·4, 26·1) cm, respectively. Each piezoceramic patch was 25 mm × 25 mm × 1 mm and weighed 6·3 g. For measuring the plate responses, one of the piezoceramic patches was used as an actuator to excite the plate and an accelerometer (B&K 4393), weighing 2·2 g, was used as an acceleration sensor. Figure 8 shows the experimental setup.

TABLE 2

The fundamental data for reverberant room

Reverberant room	Volume (m^3)	Inner surface area (m^2)	Reverberant time (s)			
			200 Hz	315 Hz	400 Hz	500 Hz
–	205·6	216·8	14·6	14·2	12·6	11·6

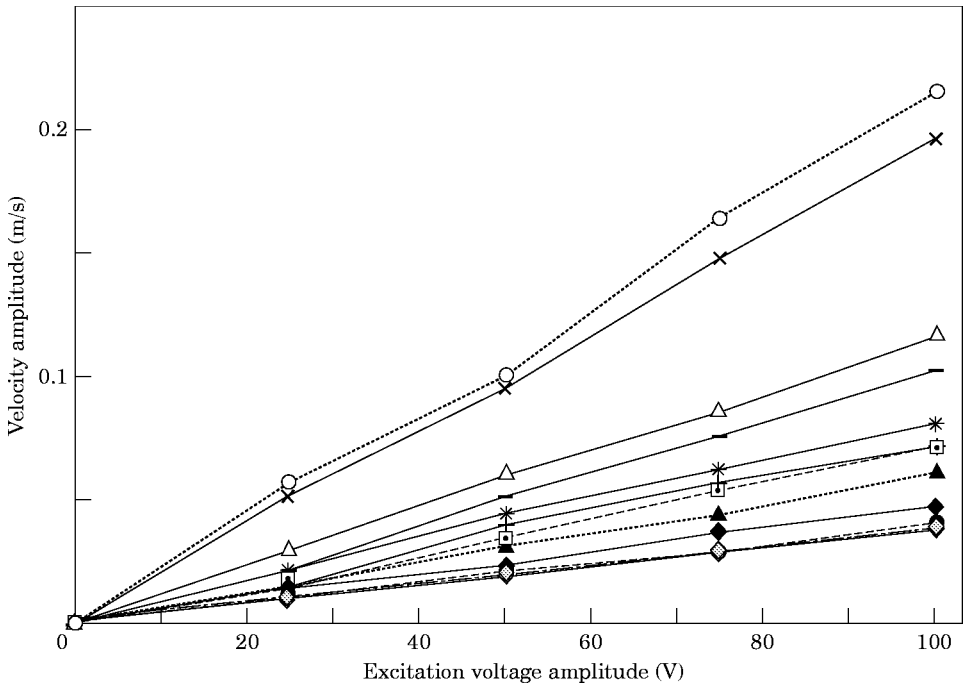

Figure 10. The proportionality between plate velocity amplitude and the piezoactuator excitation voltage ε_{PZT}. Key for actuator location (x, y) for various frequencies (Hz). (12, 14·6): —○—, 214·45; —×—, 319; —+—, 389; —◇—, 489. (5·8, 26·7) —◆—, 214·45; —*—, 319; —▬—, 389; —⊡—, 489. (32·1, 27·4); · ·△· ·, 214·45; · ·●· ·, 319; · ·◇· ·, 389; —△—, 489.

In the previous calculations of sound radiation power, only the upper semi-finite space has been taken into consideration. The arrangement, shown in Figure 7, was hence baffled and placed at the opening of the anechoic chamber (Figure 9). The power radiated from the back of the plate can be completely absorbed by such an arrangement. In the first part of the measurements, the original baffle of the plate on the opening of the anechoic chamber was 0·8 cm thick plywood. In the second part of the measurements, the original baffle was replaced by 2 cm thick plywood in order to prevent the part of sound power from penetrating into the anechoic chamber from the reverberant room. All the gaps were well sealed by acoustic absorbing material.

The measurements of the radiation power, following ANSI-S1.21-1972 [10] specifications, were conducted by placing the anechoic chamber in the reverberant room.

TABLE 3

Coupling coefficient k_0 for the piezoceramics for various frequencies

Mode (frequency)	1 (106)	2 (214·45)	3 (319)	4 (389)	5 (489)
Coupling coefficient k_0 (Nt-m/volt)*10^{-4}	7·199	30·31	35·99	28·75	27·56

After measuring the pressure level L_i for all the required positions in ANSI, the average sound pressure level L_p was calculated as

$$L_p = 10 \log \left[\frac{1}{N_m} \sum_{i=1}^{N_m} \log^{-1} \left(\frac{L_i}{10} \right) \right]. \tag{34}$$

From equation (34) the sound power level L_W was then obtained as

$$L_W = L_p - 10 \log (T) + \log (V_r) + 10 \log (1 + S_r \lambda / 8 V_r) + 10 \log (B/1000) - 14, \tag{35}$$

where V_r is the volume of reverberant room, N_m is the number of microphones, S_r is the total area of the inside surface of the reverberant room, T is the echo time, λ is the wavelength, and B is the atmospheric pressure (mb). According to ANSI, the reference pressure level and sound power are $20\,\mu\mathrm{N/m^2}$ and 10^{-12} Watt respectively. The fundamental data of the reverberant room is given in Table 2 [11].

5. RESULTS AND COMPARISONS

The calculated and measured resonant frequencies for the first six modes are listed in Table 1. The accuracy of the present method was shown by comparison with the results obtained by the Rayleigh–Ritz method. It can be easily seen that the present method offers a much more simplified approach to obtaining the response of a rectangular plate under a variety of boundary conditions. Moreover, the comparison also shows that the fixed boundary in the experimental setup is close to ideal and the influence of the attached piezoceramic patches is almost negligible.

From equations (24) and (25) is can be observed that the plate displacement $W(x, y)$ is proportional to the applied moment $\mathbf{M}$. That is

$$W(x, y) = \mathbf{M} G(\xi_0, \eta_0, x, y). \tag{36}$$

Substituting equation (36) into equation (15) the relation velocity and input moment can be obtained as

$$V(x, y) = \omega \mathbf{M} G(\xi_0, \eta_0, x, y). \tag{37}$$

Equation (37) indicates that the velocity amplitude is proportional to the moment $\mathbf{M}$.

In order to verify the proportionality between $\mathbf{M}$ and ε_{PZT}, 25, 50, 75 and 100 V harmonic voltages were applied to piezoceramic 1 successively. The velocity amplitudes at three different points A(12, 14·6) cm, B(5·8, 26·7) cm and C(32·1, 27·4), cm were measured and are plotted in Figure 10. It can be seen from Figure 10 that such proportionality indeed exists for each individual mode, confirming the validity of the relation $\mathbf{M} = k_0 \varepsilon_{PZT}$. The coupling coefficient k_0 can thus be determined by comparing equation (37) and the measurement results. Equation (38) gives the coupling coefficient k_0 by setting the harmonic exciting voltage for the piezoceramic 1 to 141·4 V:

$$k_0 = V_2 / 141{\cdot}4 \times V_1. \tag{38}$$

Table 3 gives the coupling coefficient k_0 for the first five modes.

From equation (24) the mode shapes are calculated by using 20×20 terms. Piezoceramic 1 is used as actuator and the excitation moment is $\mathbf{M} = 1$ nt $-$ m (Figure 11). The pictures for these corresponding mode shapes are taken by spreading sand on the surface of the vibrating plate. The lines in Figure 12 are the nodal lines corresponding to each mode. For comparison, the vibration amplitudes are also measured by using the accelerometer on the plate and the results are shown in Figure 13.

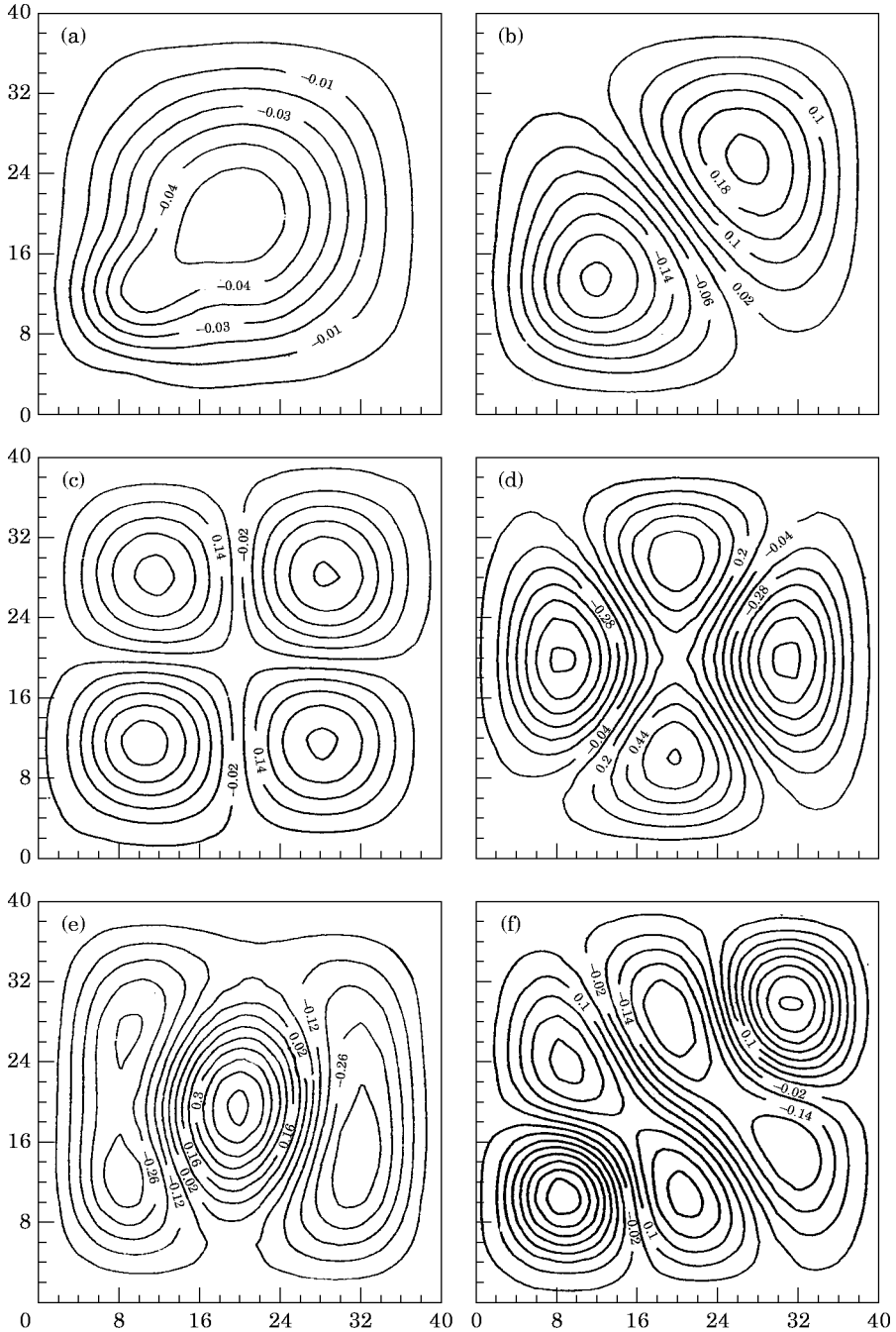

Figure 11. Simulation of plate responses (m/s) under excitation by piezoceramic 1. (a) first mode (106 Hz); (b) second mode (214·45 Hz); (c) third mode (319 Hz); (d) fourth mode (389 Hz); (e) fifth mode (390·8 Hz); (f) sixth mode (489 Hz).

The plate was divided into 20×20 elements for the calculation of the radiated sound power. The results of calculated and measured radiated sound power are given in Table 4. The analytical results are obtained by using equation (33), considering 141·4 V harmonic as exciting voltage for piezoceramic 1.

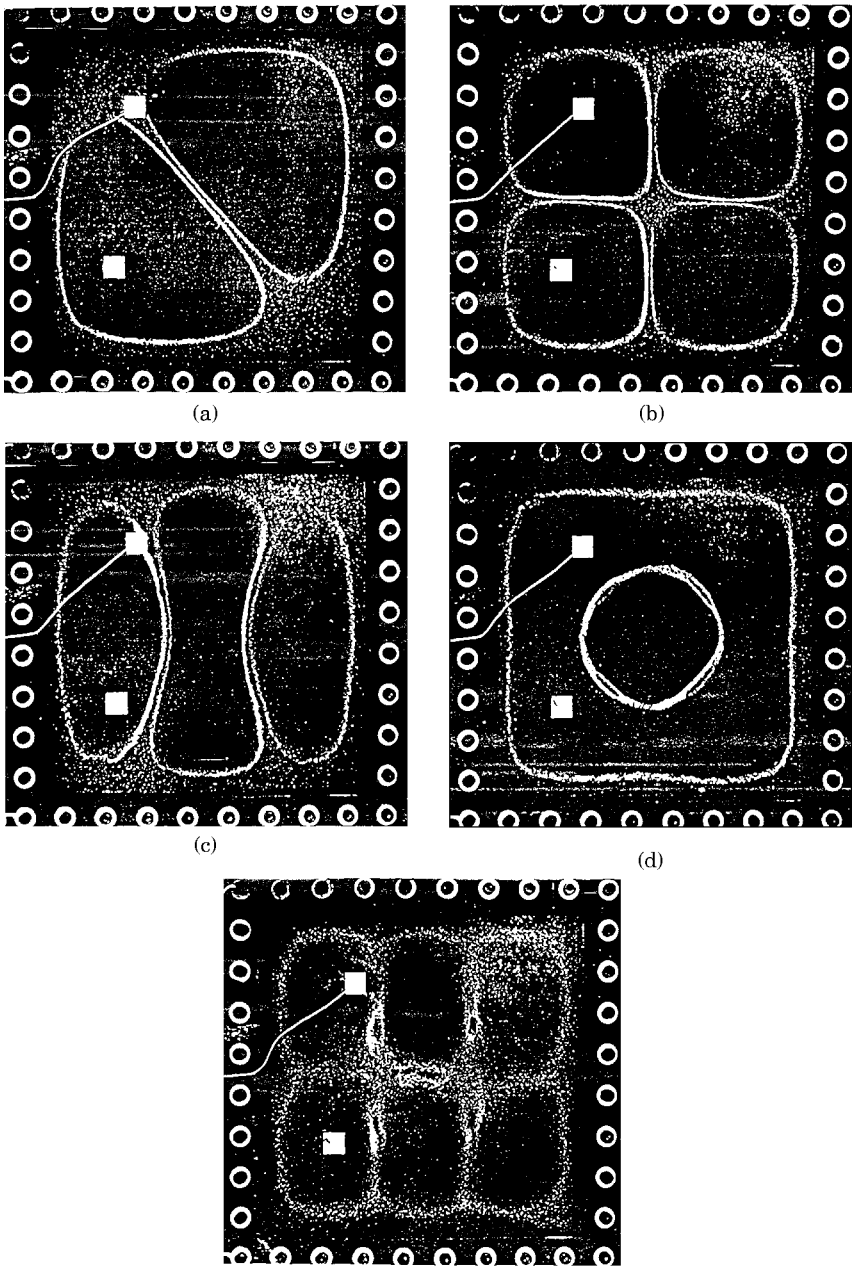

Figure 12. Picture of plate responses (m/sec) under excitation by piezoceramic 1. (a) second mode (214·45 Hz); (b) third mode (319 Hz); (c) fourth mode (389 Hz); (d) fifth mode (390·8 Hz); (e) sixth mode (489 Hz).

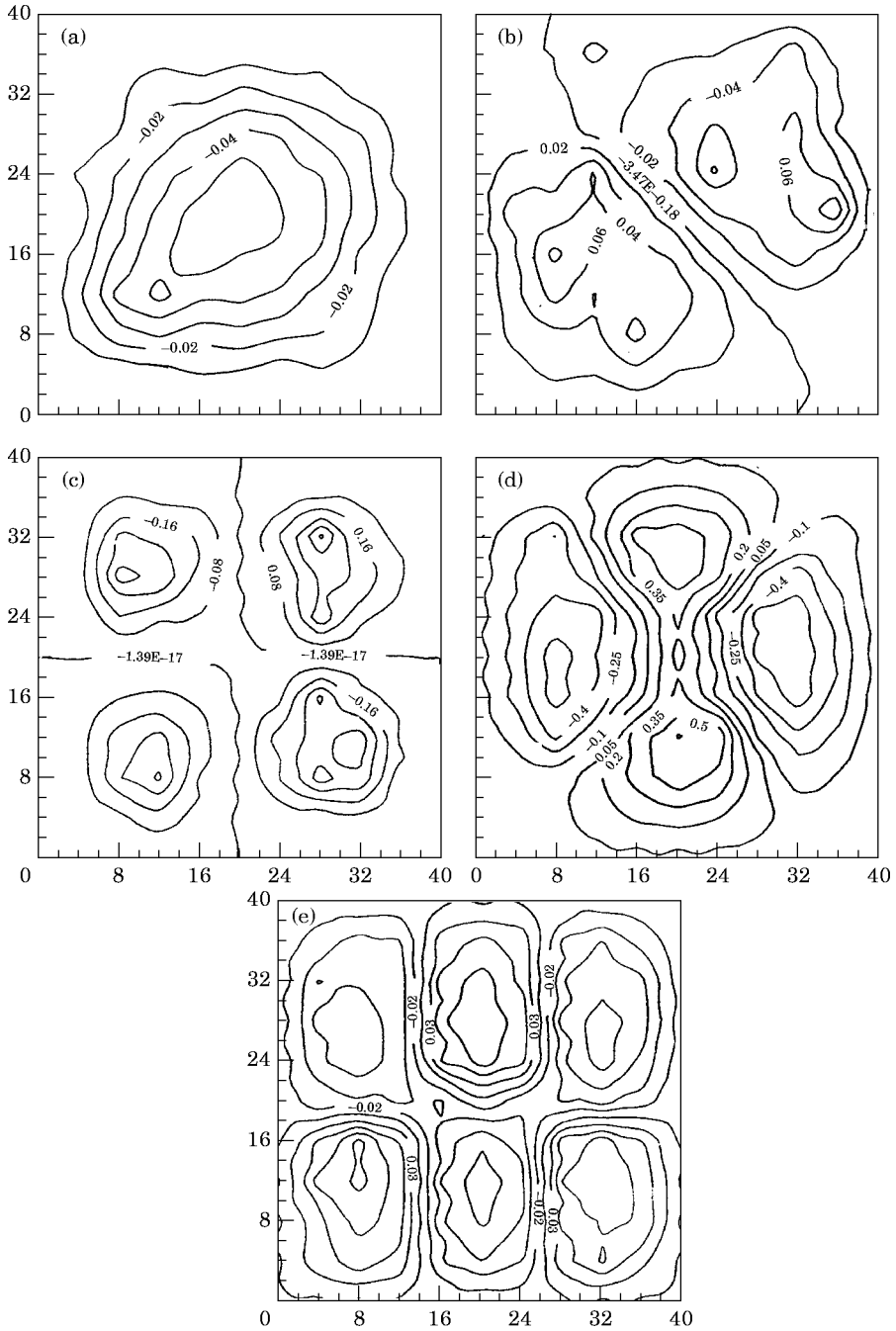

Figure 13. Experimental measurements of plate responses (m/s) under excitation by piezoceramic 1 with excitation voltage $\varepsilon_{PZT} = 141{\cdot}4$ V. (a) first mode (106 Hz); (b) second mode (214·45 Hz); (c) third mode (319 Hz); (d) fourth mode (389 Hz); (e) fifth mode (489 Hz).

TABLE 4

Comparison between the calculated and measured sound power radiated by the plate

	Actuator		Sound power (dB)		
Mode (frequencies)	ε_{PZT}	$\mathbf{M}_e$	calculated	measured (original baffle)	measured (improved baffle)
2 (214·5)	141·4	0·429	90·4	86·2	88·6
3 (319)	141·4	0·509	91·5	82·4	85·8
4 (389)	141·4	0·406	107·5	92·4	100·7
6 (489)	141·4	0·389	104·9	94·3	98·3

6. DISCUSSION AND CONCLUSION

A novel method for the analysis of the plate response with clamped boundary condition and plate radiated sound power has been presented. The response and radiated sound power of a plate subjected to four point moments excitation which simulates a piezoceramic actuator has been obtained by this method and compared with the experimental results in order to confirm the accuracy of the results. Measurement of radiated sound power in the reverberant room with an anechoic chamber is also shown to be an alternative and economic approach.

The possible reasons responsible for the minor deviations between the calculated and measured radiated sound power may be listed as follows:

1. For the monotonous frequencies below 500 Hz the sound field does not have perfectly uniform distribution in the reverberant room due to the lack of a diffuser.
2. The reverberant environment gets slightly distorted due to the existence of the anechoic chamber in the reverberant room.
3. The baffle on the opening of the anechoic chamber is not perfect for frequencies below a few hundred Hz. A part of the radiated sound power may hence get transmitted through the baffle and is absorbed by the anechoic chamber, thus lowering the measured value. It may be noted that the accuracy of the measurement was observed to increase after the baffle was improved.

Furthermore, the model presented in this paper is particularly convenient when active control of plate response, sound radiation and sound transmission are desired, since all the information, e.g., the dynamics of the structure, required for the control can be obtained and is present in the structure, i.e., the plate, itself.

ACKNOWLEDGMENT

The authors would like to acknowledge the National Science Council, Taiwan, R.O.C. for the partially funding support under project no. NSC 83-0209-E-002-010.

REFERENCES

1. G. B. WARBUTON 1954 *Proceedings of Institute of Mechanical Engineers* **168**, 371–381. The vibration of rectangular plates.
2. R. SZILARD 1966 *Theory and Analysis of Plates*, *Classical and Numerical Methods*. New Jersey: Prentice-Hall; 435.
3. N. LI 1992 *Journal of Sound and Vibration* **158**, 307–316. Forced vibration analysis of the clamped orthotropic rectangular plate by the superposition method.

4. V. Z. Vlasov 1949 *Nat. Adv. Comm. Aeron., Naca Technical Memo* **1024**, Some new problems on shell and thin structures.
5. L. Rayleigh 1987 *Theory of Sound* (two volumes). New York: Dover Publications; second edition, 1945 re-issue.
6. E. F. Crawley and de Luis Javier 1987 *American Institute of Aeronautics and Astronautics Journal* **25**, 1373–1385. Use of piezoelectric actuators as an element of intelligent structures.
7. R. L. Clark, C. R. Fuller and A. Wicks 1991 *Journal of Acoustics Society of America* **90**, 346–357. Characterization of multiple piezoelectric actuators for structural excitation.
8. K. Naghshineh and G. H. Koopman 1992 *Journal of Acoustic Society of America* **92**, 856–870. A design method for achieving weak radiator structures using active vibration control.
9. W. Flugge 1962 *Handbook of Engineering Mechanics*. New York: McGraw-Hill.
10. American National Standard Institute 1972 *Methods for the Determination of Sound Power Level of Small Sources in Reverberation Rooms*. Acoustical Society of America.
11. Department of Naval Architecture and Ocean Engineering, National Taiwan University, 1988 *Introduction of Noise and Acoustic Laboratory*.